Generalized Dynamic Simulation of Skid in Ball Bearings

Pradeep K. Gupta*
Mechanical Technology Inc., Latham, N.Y.

A new analysis for determining skid in ball bearings is presented in terms of a generalized integration of the differential equations of motions of the ball under prescribed traction-slip relationship at the ball race contacts. The analytical formulation is free of assumptions like "race control" or "no gyroscopic slip" and the ball motion is defined in the generalized six degrees of freedom system. Based on the nature of available elastohydrodynamic traction data, a traction-slip relationship is postulated and the motion of the ball is examined when one of the races is subjected to an angular acceleration. The solutions predict both the magnitude of slip velocities and the expected wear rates for a prescribed wear coefficient. Influence of preload is examined and the capability of the present formulation in determining the required preload to prevent skidding is demonstrated. The computer program developed to obtain the time dependent ball motion is introduced as an up-to-date design tool in predicting skid and ball motion as a whole in angular contact ball bearings.

Nomenclature

a = length of semimajor axis of contact ellipse, in.
A = dimensionless semimajor axis
b = length of semiminor axis of contact ellipse, in.
B = dimensionless semiminor axis
d = ball diameter, in.
D = dimensionless ball diameter
$\mathbf{F}$ = applied force vector, lb
$\mathbf{F}^*$ = dimensionless applied force vector
$\mathbf{G}$ = applied moment vector, in.-lb
$\mathbf{G}^*$ = dimensionless moment vector
I = ball moment of inertia, lb-in.-sec^2
K = wear coefficient
m = mass of the ball, lb-sec/in.^{2}
p_H = maximum Hertz pressure, lb/in.^{2}
Q = ball race contact load, lb
Q_0 = static ball-race contact load, lb
R = dimensionless radial position
r_e = pitch radius, in.
r_o = characteristic length, in.
t = time, sec
$\mathbf{u}$ = slip velocity vector, in./sec
W = wear rate, in.^{3}/sec
τ = dimensionless time

Coordinate Frames

(x, r, η) = inertial frame
$(\hat{x}, \hat{y}, \hat{z})$ = ball frame
(x, y, z) = coordinate frame along the contact load
(ξ, ζ) = axes in the contact ellipse

I. Introduction

THE increasing speeds and severity of operating conditions of modern high speed propulsion systems has resulted in a substantial interest in the dynamics of rolling element bearings generally used in these advanced applications. Most of the kinematic treatments of ball bearings until recently have been limited to the hypotheses of inner or outer race control postulated by Jones[12,13] and, thus, the ball angular velocity vector is clearly defined and a quasi-static force balance type of calculation is carried out to estimate the bearing behavior. Based on such simplified hypotheses, Poplawski and Mauriello[15] presented a simple analysis for predicting skidding in angular contact ball bearings.

Harris[7] has recently proposed that race control is generally valid for high-speed bearings when the traction coefficient at the ball race contacts is high enough to prevent any gyroscopic slip. Also, in his later work[8] it has been pointed out that these simple kinematic hypotheses do not hold under elastohydrodynamic conditions. With a very simple elastohydrodynamic traction model, Harris[8] has modified the existing force balance type of analysis to avoid the use of race control theories. The convergence of the solution of the nonlinear equations in such a modified quasi-static analysis will strongly depend on the traction-slip characteristics. Furthermore, in applications where the balls are continuously accelerating and decelerating a force balance type of computation may be quite meaningless.

A dynamic formulation of motion of the various bearing elements has been presented by Walters.[18] This work is basically concerned with the dynamics of the separator and a constrained ball motion is assumed. Nevertheless, the resulting differential equations of motion are integrated to obtain the true motion. The constraints on the ball motion require that the contact angles and loads as a function of the orbital position of the ball are predetermined by a simple conventional quasi-static analysis where the effects of centrifugal forces have been included. Thus, the contact angles and loads are not influenced by any dynamics of the bearing elements. It is clear that this assumption will not hold if the bearing is subjected to dynamic variations in applied load or accelerations of the races and hence the formulation cannot be used for investigating skid and other transient phenomenon in ball bearings. Furthermore, in a lubricated bearing validity of a constrained motion, established by quasi-static methods of Jones,[12,13] is still questionable and a generalized solution of the ball motion in a six-degree-of-freedom system is necessary.

Although substantial advancements have been made in understanding the lubrication mechanics at ball-race contacts, formulation of a general lubrication model as required in the dynamics of rolling element bearings still needs a considerable research. The classical Dawson and Higginson's Theory[4] for computing lubricant film thickness in cylinderical elastohydrodynamic (EHD) contacts has been modified by Cheng[2,3] to include the thermal effects and side leakage in elliptical contacts. A substantial experimental work has also been reported in this area as compiled by McGrew et al.[14] Allen et al.[1] have performed experiments with a spinning ball under lubricated conditions. Experimental rheological data for some lubricants are also available.[11,16,17] Based on these experimental

Received May 21, 1974; revision received October 7, 1974.
Index categories: Structural Design, Optimal; Structural Stability Analysis.
*Senior Engineering Scientist.

findings, some attempts have been made to derive semi-empirical traction models.[6,16]

The primary objective of this paper is to integrate the generalized differential equations of motion for a ball in a thrust loaded angular contact bearing under realistic operating conditions. The motion is considered with the six degrees of freedom and it is shown that these equations may be integrated with arbitrary traction-slip relation and any set of initial conditions. Steady-state solutions with constant but fairly low traction coefficient are compared with those obtained by simple quasistatic force balance type of analyses. Based on the qualitative nature of most of the available lubricant rheology data, a simple algebraic correlation is used to simulate a traction model. Under such simulated conditions, skid in the bearing is examined as the rotating race is subjected to an acceleration. The effects of the applied thrust load on bearing skid are also demonstrated.

II. Equations of Ball Motion

The complete motion of the ball is obtained by considering the translational and orbital motion of the center of the mass in the cylindrical inertial coordinate frame (x,r,η) and the rotational motion of the ball about its mass center in the ball frame $(\hat{x},\hat{y},\hat{z})$ as shown in Fig. 1. Generally the $(\hat{x},\hat{y},\hat{z})$ system is fixed in the body along the principal inertial axes, but if the balls are perfectly spherical any orthogonal system is equally convenient to describe the motion. Hence, $\hat{x},\hat{y},\hat{z}$ is selected such that the $\hat{z}$ axis lies along the radius vector $\mathbf{r}$ and the $\hat{x}$ axis is parallel to the inertial axis x. Denoting the mass of the ball by m and the moment of inertia by I, the equations of motion are described as:

$$\begin{aligned} m\ddot{x} &= F_x \\ m(\ddot{r} - r\dot{\eta}^2) &= F_r \\ m(r\ddot{\eta} + 2\dot{r}\dot{\eta}) &= F_\eta \end{aligned} \tag{1}$$

$$\begin{aligned} I\dot{\omega}_{\hat{x}} &= G_{\hat{x}} \\ I\dot{\omega}_{\hat{y}} - I\omega_{\hat{z}}\dot{\eta} &= G_{\hat{y}} \\ I\dot{\omega}_{\hat{z}} + I\omega_{\hat{y}}\dot{\eta} &= G_{\hat{z}} \end{aligned} \tag{2}$$

where F_x, F_r, F_η denote the components of the applied force vector, $\mathbf{F}$. $G_{\hat{x}}$, $G_{\hat{y}}$, $G_{\hat{z}}$ represent the components of applied moment vector $\mathbf{G}$ and the ball angular velocity is denoted by the components $\omega_{\hat{x}}$, $\omega_{\hat{y}}$, $\omega_{\hat{z}}$. Also, the first derivatives are denoted by a dot $(\cdot)$ over the variable and the second derivative is represented by two dots. The orbital velocity of the ball is clearly η.

It should be noted that the contact forces at ball-race contact, and resulting tractive forces (with a prescribed traction-slip relation) form the applied force and moment vectors $\mathbf{F}$ and $\mathbf{G}$.

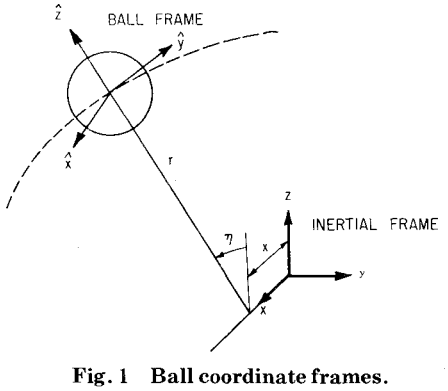

Fig. 1 Ball coordinate frames.

The normal contact forces for any prescribed position of the ball relative to the races are determined by solving the equilibrium of the races, as done in most force balance type of computations.[9] Knowing these loads, the Hertzian pressures and contact ellipses at both the outer and inner race contacts are determined. The tractive force vector $\mathbf{dF}$, over an infinitesimal area within the contact ellipse is defined by

$$\mathbf{dF}_t = \kappa(\mathbf{u})dQ \tag{3}$$

where dQ is the normal force, $\mathbf{u}$ is a vector defining the local slip velocity, and κ is defined as a local traction coefficient.

Traction coefficient κ is generally a function of slip as shown in Eq. (3), and it is this variation which constitutes a traction model which should be derived from the lubricant behavior. Most of the available experimental data shows a qualitative trend that traction initially increases with increasing slip, reaches a maximum value at some slip velocity and finally reduces to some asymptotic value as the slip increases further. Such a qualitative trend may be simulated by an expression of the form

$$|\kappa| = (\Psi_1 + \Psi_2 u)\exp(\Psi_3 u) + \Psi_4 \tag{4}$$

In general, the coefficients Ψ_1, Ψ_2, Ψ_3, and Ψ_4 will be a function of operating conditions and the lubricant properties. However, for the present investigation they are assumed to be constant and the specific values are derived from the conditions found to be in the range of available traction data. The conditions used are:

$$\begin{aligned} |\kappa| &= 0 & |u| &= 0 \\ |\kappa| &= |\kappa|_{\max} = 0.010 & |u| &= |u|_0 = 20 \text{ in./sec} \\ |\kappa| &= |\kappa|_\infty = 0.007 & |u| &= \infty \end{aligned} \tag{5}$$

With the aforementioned conditions, Eq. (4) is solved to determine the required coefficients. The resulting simulated traction model is shown graphically in Fig. 2.

The traction force vector will generally have two components; i.e., along the major and minor axes of the contact ellipse. If subscripts 1 and 2 are used, respectively, these components are defined as

$$\begin{aligned} \kappa_1 &= |\kappa| u_1/|u| \\ \kappa_2 &= |\kappa| u_2/|u| \\ dF_{t_1} &= \kappa_1 dQ \\ dF_{t_2} &= \kappa_2 dQ \end{aligned} \tag{6}$$

Equation (3) should in general be integrated over the elliptical contact area to determine the total tractive force.

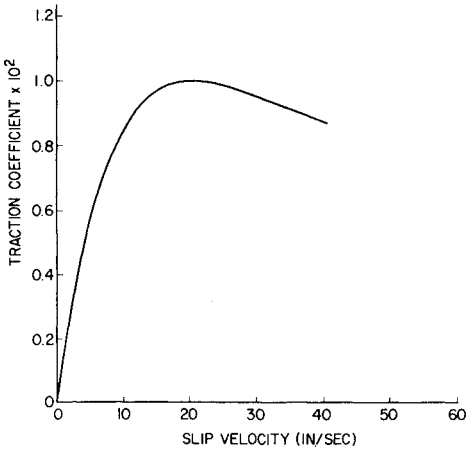

Fig. 2 Simulation traction model for ball-race lubricated contact.

However, for most bearing geometries it is found that the length of the minor axis is about four to five times smaller than that of the major axis. Under such conditions it is reasonable to neglect the variations in slip along the minor axis. Denoting the axes of the ellipse as shown in Fig. 3, the normal load for the indicated infinitesimal area is determined from the Hertzian pressure distribution.

$$dQ = \frac{\pi}{2} p_H ab(1 - \bar{\xi}^2)d\bar{\xi} \tag{7}$$

where $\xi = \xi/a$ and the Hertzian parameters p_H, a, and b are as defined in the nomenclature.

The slip velocity vector is now computed only along the major axis of the contact ellipse. This computation is quite forward, although it involves a substantial algebraic manipulation. The velocities of the race and the race are primarily transformed to the coordinate frames of the contact ellipse and the slip vector is determined. The total tractive force is determined by integrating Eq. (3) numerically. The normal force combined with the tractive force represent the net applied force vector at a ball-race contact.

Moment vector about the ball center is computed by a vector cross product of the position vector locating the center of the infinitesimal area in the contact ellipse and the net force acting on this area. The resulting increment vector is again integrated numerically to obtain the total moment vector. The force and moment vectors computed as described above are transformed in proper coordinate frames as required by Eqs. (1) and (2). The formulation of the differential equations of motion now becomes complete. Since integration is performed numerically, it is necessary to nondimensionalize these equations. This is accomplished by defining the following dimensionless variables

$$X = x/r_o \qquad R = (r - r_e)/r_o$$

$$F_i^* = F_i/Q^o P_i^* A_i^* B_i^* \qquad G_i^* = G_i/Q^o r_o P_i^* A_i^* B_i^*$$

$$\tau = t(Q^o/mr_o)^{1/2} \qquad \Omega = \omega(mr_o/Q^o)^{1/2}$$

$$P_i^* = p_{H_i}/p_H{}^o \qquad A_i^* = a_i/a^o$$

$$B_i^* = b_i/b^o \qquad R_e = r_e/r_o$$

$$D = d/r_o \tag{8}$$

where Q^o is the static normal ball-race contact load, r_e is the pitch radius, r_o is a characteristic length assumed to be the radius of the ball in this paper, and the subscript i is used to denote the races (i = 1 represents outer race and i = 2 denotes inner race). The selection of scaling Hertzian parameters $p_H{}^o$, a^o, and b^o is arbitrary, and the static values at the outer race contact are used. With the previous definitions and assuming the ball to be perfectly spherical (moment of inertia $I = md^2/10$), Eqs. (1) and (2) are reduced to dimensionless forms

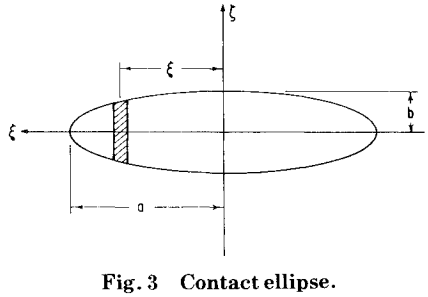

Fig. 3 Contact ellipse.

Table 1 Comparison of steady-state dynamic solution with the available quasi-static solution

Parameter		Quasi-static force balance computation	Dynamic analysis with traction coeff. = 0.007
Ball angular velocity (rpm)	ω_x	57,670	57,950
	ω_y	0	121
	ω_z	3 591	580
Ball orbital velocity (rpm)		7 255	7 247
Spin-to-roll ratio	outer race	0	0.0823
	inner race	0.689	0.754
Contact angle (deg)	outer race	4.074	5.358
	inner race	37.70	37.51
Contact load (lb)	outer race	109.9	108.9
	inner race	17.21	17.29

$$d^2X/d\tau^2 = \sum_{i=1}^{2} F_{x_i}{}^* P_i^* A_i^* B_i^*$$

$$d^2R/d\tau^2 - (R_e + R)(d^2\eta/d\tau^2) = \sum_{i=1}^{2} F_{r_i}{}^* P_i^* A_i^* B_i^*$$

$$(R + R_e)(d^2\eta/d\tau^2) + 2(dR/d\tau)(d\eta/d\tau) = \sum_{i=1}^{2} F_{\eta_i}{}^* P_i^* A_i^* B_i^* \tag{9}$$

and

$$d\Omega_{\bar{\xi}}/d\tau = 10/D^2 \sum_{i=1}^{2} G_{\bar{\xi}}{}^* P_i^* A_i^* B_i^*$$

$$d\Omega_{\bar{\eta}}/d\tau - \Omega_{\bar{\zeta}}(d\eta/d\tau) = 10/D^2 \sum_{i=1}^{2} G_{\bar{\eta}}{}^* P_i^* A_i^* B_i^*$$

$$d\Omega_{\bar{\zeta}}/d\tau + \Omega_{\bar{\eta}}(d\eta/d\tau) = 10/D^2 \sum_{i=1}^{2} G_{\bar{\zeta}}{}^* P_i^* A_i^* B_i^* \tag{10}$$

A fourth-order Runga-Kutta-Merson method[5] is used to integrate the equations of motion. This scheme requires an additional evaluation of the derivatives at each time step to estimate the truncation error. Thus, a test on convergence of the obtained integrated solutions is possible.

III. Results

A typical angular contact bearing is selected arbitrarily to obtain numerical solutions of the above system of differential equations of motion. The geometry of the selected bearing is defined by the following parameters: number of balls = 19; factor = 0.52; ball diameter = 0.59375 in.; pitch diameter = 4.13390 in.; and contact angle = 25°.

For the purpose of comparing the steady-state solutions with the solutions obtained by simple force balance type of quasi-static computations, the bearing is assumed to be operating with a 200 lb thrust load and inner race rotating at 15,000 rpm. These solutions are very similar to those obtained by Jones[12,13] and Harris.[8] The initial conditions for the dynamic analysis are determined by the outer-race control solution and a constant traction coefficient of 0.007 is assumed. Under such conditions if the steady-state dynamic solution and the outer race control quasi-static solution are closely the same, then very small accelerations of the ball will result. However, it is found that with such a low traction coefficient gyroscopic slip of the ball is possible and the steady-state solution is substantially different from the outer race control solution where no gyroscopic slip is allowed. The solutions are compared in Table 1. It is clearly seen that a large gyroscopic slip develops and the ball angular velocity vector ends to become parallel to the bearing axis. Harris[8] has reported similar findings from his quasi-static analysis. Also, Hira-

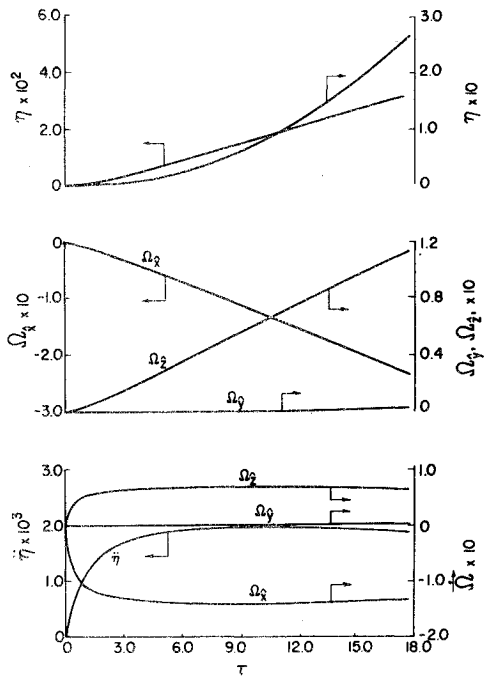

Fig. 4 Dimensionless solution for 200-lb thrust load. Inner race accelerating at 50,000 rpm/sec.

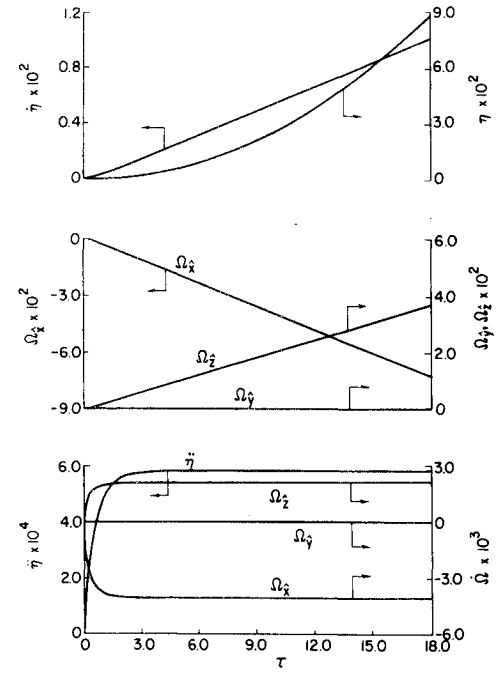

Fig. 5 Dimensionless solution for 800-lb thrust load. Inner race accelerating at 50,000 rpm/sec.

no[10] has presented experimental evidence of such a behavior. The most interesting solutions are found when the race is accelerating. Such a condition is relevant in case of start-stops or acceleration to operating speed from the idle speed. Under such transient conditions, significant skid may be developed in the bearing. The dynamic analysis presented here simulated such a dynamic behavior in an elegant manner when the traction is determined by the hypothetical model shown in Fig. 2. With a 200-lb thrust load and static condition, the inner race of the bearing is accelerated at the rate of 50,000 rpm/sec. The equations of ball motion are integrated with these conditions and the results are shown in Fig. 4 in dimensionless form. Since the traction coefficients levels off to an asymptotic value with increasing slip, the ball soon develops fairly constant accelerations. A steady increase in the components $\Omega_{\hat{x}}$, $\Omega_{\hat{z}}$, and the orbital velocity $\dot{\eta}$ is clearly seen in Fig. 4. There is also a gradual increase in the component $\Omega_{\hat{y}}$, however, the rate of change is small because this is directly related to the gyroscopic moment. Similar solutions are also obtained with the thrust load increased to 800 lb as shown in Fig. 5. Since the time scale is inversely proportional to the static ball load [see Eq. (8)], it is expected that the time for initial transients will be reduced by a factor of two when the applied load is increased from 200 to 800 lb. This is indeed observed by comparing Figs. 4 and 5.

The contact loads and dynamic forces and moments on the ball are plotted as a function of time in dimensional form in Fig. 6. It is clearly seen that as the race speed increases, the ball accelerates and increases in centrifugal force results in a decreasing contact angle at the outer race. The contact load also increases. At the inner race, as might be expected, the contact angle increases and the load decreases. Magnitudes of gyroscopic moments are also shown in Fig. 6. The solutions for the 200-lb thrust load, shown in the lower half of Fig. 6, are compared with those obtained with a 800-lb thrust load shown in the upper half of the diagram.

Ball angular velocities for the two cases are compared in Fig. 7. It is interesting to see that the ball motion starts in a mode close to inner race control but very rapidly the spin-to-roll ratios on ball races become almost equal as the ball continues to accelerate. It is expected that as the ball velocities increase to the steady state mode the spin to roll ratio on the outer race will increase and if the traction coefficients are high enough to prevent gyroscopic slip, the solution will tend towards an outer race control mode. Bearing skid under such dynamic conditions is generally defined by variation in a parameter λ, which is a

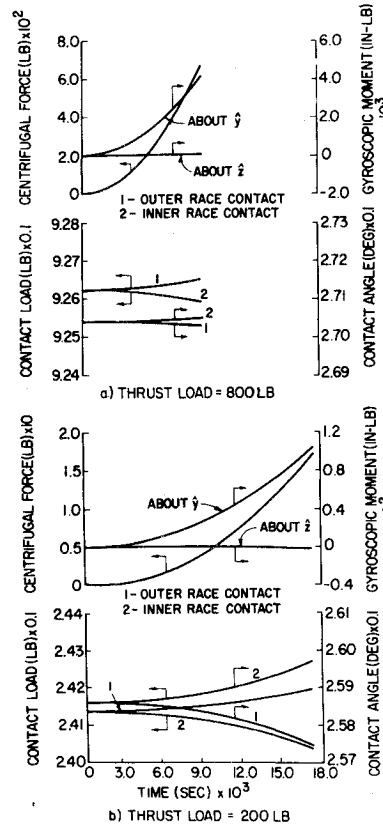

Fig. 6 Comparison of ball loads and moments for the 200-lb and 800-lb applied thrust loads.

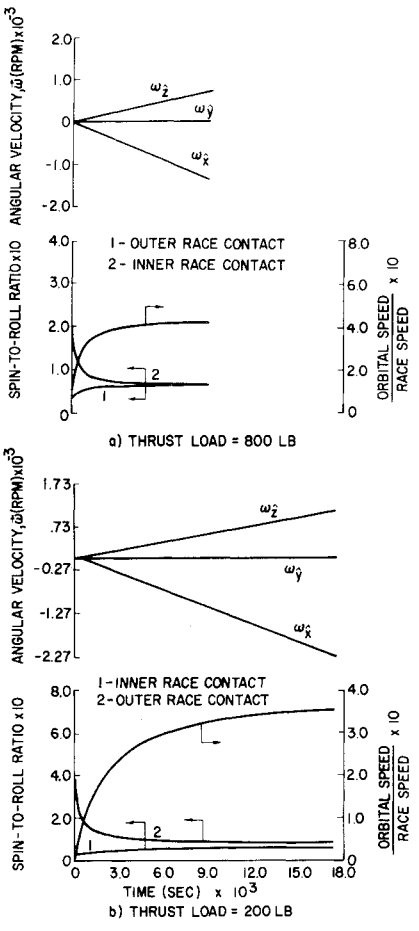

Fig. 7 Comparison of ball velocities in case of the 200-lb and 800-lb thrust loads.

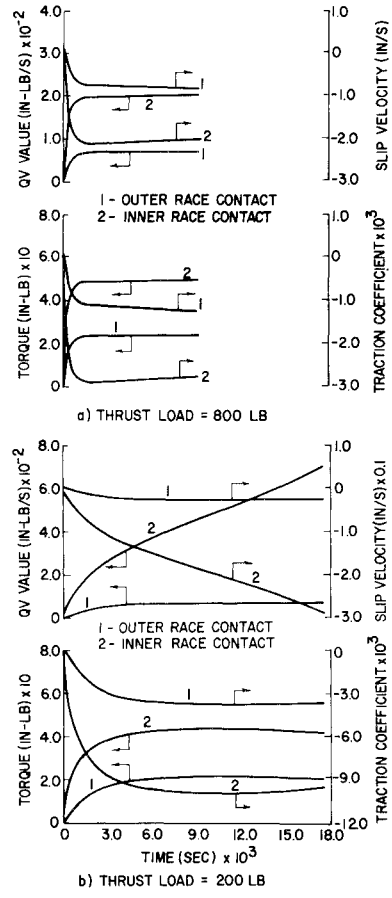

Fig. 8 Variations in slip, bearing torque, traction coefficients and QV values in case of the 200-lb, and 800-lb thrust loads.

ratio of ball orbital velocity to the rotational velocity of the race.

$$\lambda = \frac{\text{orbital velocity of the ball}}{\text{angular velocity of rotating race}} \tag{11}$$

The variations of this parameter are also shown in Fig. 7. It is clearly seen that the time required to overcome the initial transients is much smaller with the 800-lb load than that in the 200-lb case. This signifies a lesser extent of skidding with the increased thrust load as might be expected. The severity of skidding is seen more clearly in Fig. 8 where the slip velocity in the center of contact and along the rolling direction are plotted. It is seen that at the inner race contact the slip with a 200-lb thrust load has reached a value of about 30 in./sec in 18 msec and it is still increasing while the slip with 800 lb load reaches a maximum value of only about 2 in./sec and it has already begun to reduce in a time of only about 3 msec. Slip rates at the outer race contact will be generally small since only the inner race is accelerating in this case. This is also seen in Fig. 8. The component κ_2 of the traction coefficient in the rolling direction are also plotted in Fig. 8. The negative signs just correspond to the direction of slip, which is plotted in Fig. 8 as the velocity of the race relative to the ball. It is interesting to see that in spite of increasing the applied thrust load from 200 to 800 lbs, there is only a small increase in the torque on the races. The explanation to this directly lies in the fact that the traction coefficients are quite lower, due to lesser skidding, in the case of a 800-lb thrust load as clearly seen in Fig. 8.

From a design standpoint, it becomes important to determine the wear due to such accelerations and resulting skid in the bearing. Based on the steady accelerations and roughly estimating the final steady-state motion, the time required to reach steady state can be easily estimated. Thus if the wear rate during acceleration is determined, the total wear in an acceleration cycle may be determined. This will help determine the number of start-stops or relevant accelerations which the bearing can survive before it has worn excessively. These wear rates are determined by a QV value which is defined by the integral over the contact ellipse of the product of normal load and the absolute slip velocity. From the classical wear theories, wear rate is primarily expressed in terms of the relation

$$W = (KQV/H) \text{ in.}^3/\text{sec} \tag{12}$$

where W = wear rate (in.^{3}/sec); K = wear coefficient; Q = normal load (lb); V = sliding velocity (in./sec) and H is the hardness of the material (lb/in.^{2}). Applying Eq. (12) incrementally over the contact ellipse the wear rate is expressed as

$$W = (K/H)\int_{-1}^{1} u(\bar{\xi})Q(\bar{\xi})d\bar{\xi} \tag{13}$$

where $Q(\xi)\,d\xi = dQ$ is the load over an infinitesimal area and the integration is performed over the entire contact ellipse.

It is the value of the previously mentioned integral which is denoted as the QV value in Fig. 8. Symbolically

$$QV = \int_{-1}^{1} u(\bar{\xi})Q(\bar{\xi})d\bar{\xi} \tag{14}$$

Thus the results shown in Fig. 8 may be readily used to compute the expected wear due to skidding if the hardness of the material is known and the wear coefficient is approximate. It should be noted that, in general, the wear coefficient may depend on the load and rolling and sliding velocities since these factors influence the elastohydrodyn-

amic film thickness. Also, it should be recognized that skidding may not always result in wear and much more additional work is necessary for a better understanding of the factors that result in wear when skidding occurs. Thus, prediction of wear based on the QV values should only be treated as a first approximation. With due recognition to these factors, if the QV values for the two cases shown in Fig. 8 are compared, it is seen that the probable wear rate at the inner race with the 200-lb load is several orders of magnitude larger than that with the 800-lb applied load. In fact, the QV value for the lighter load is continuously increasing during the time for which solutions are plotted in Fig. 8. In general, an optimum thrust load will be determined by a compromise between wear and fatigue for prescribed operating conditions for a bearing. The proposed analysis and the computer program developed during the present investigation thus becomes a practical design tool for bearing selection or design against excessive wear due to skidding in applications where the races are subjected to accelerations or retardations. The study of the transient solutions due to any given acceleration rate of the rotating race(s) as a function of applied thrust load will provide a relationship between wear due to skidding and the applied load. This realistic relationship will replace the more simplified relation used by Poplawski and Mauriello[15] in their model for designs against skid.

Under more realistic lubrication conditions, than those determined by the hypothetical model used in this paper, it will only be necessary to replace Eq. (4) by appropriate lubrication model. The author expects to present some results based on such sophisticated traction models, derived from existing lubricant data, in the very near future.

IV. Summary

A dynamic analysis in terms of differential equations of motion is presented to analyze the transient ball motion in angular contact ball bearings under simulated EHD traction conditions at the ball-race contacts. The generalized differential equations of motions are solved with prescribed initial conditions and hence the analysis is free of simplified, and sometimes controversial, kinematic hypotheses; e.g., inner or outer race control. It is shown that large discrepancies between the general motion and the simplified motion obtained by outer race control assumption exist when the traction coefficient is low enough to allow gyroscopic slip. In fact, the ball angular velocity vector tends to become parallel to the bearing axis under such conditions.

The generalized dynamic analysis and the computer program developed in this investigation is presented as a design tool for applications where the bearing is subjected to skid due to acceleration of the races. Two typical examples of start-up are considered and it is demonstrated that the formulation not only estimates the expected wear during skid but also provides a means to determine the required preload for reducing excessive skid. In summary, a complete analysis for both the steady-state and transient ball motion is presented under prescribed operating conditions.

V. Recommendations

A generalized ball bearing dynamics program should be capable of treating both the motions of ball and the cage. The dynamics program developed in this paper does not treat the cage mechanics, whereas the available programs which do consider cage dynamics[18] assume a simplified constrained motion of the ball. Therefore, it is recommended that the present analysis be extended to include the cage dynamics. Skidding is generally quite prominent in roller bearings; however, the formulation of generalized equations of motion of the roller under realistic traction conditions is still far from complete. Such a formulation will provide a roller dynamics program similar to the one presented here for ball bearings. A final step will be to couple the roller dynamics with the dynamics of cage to obtain a generalized roller bearing dynamics program. It is expected that these proposed advancements will not only provide a major contribution to the rolling element bearing technology but will also provide the designers with the most up-to-date design and diagnostic tools.

References

[1] Allen, C. W., Townsend, D. P., and Zaretsky, E. V., "Elastohydrodynamic Lubrication of a Spinning Ball in a Nonconforming Groove," *ASME Transactions, Journal of Lubrication Technology,* Series F, Vol. 92, 1970, pp. 89–96.

[2] Cheng, H. S., "Calculation of Elastohydrodynamic Film Thickness in High Speed Rolling and Sliding Contacts," MTI Rept. 67TR24, 1967, Mechanical Technology, Inc. Latham, N.Y.

[3] Cheng, H. S., "A Numerical Solution of the Elastohydrodynamic Film Thickness in an Elliptical Contact," *ASME Transactions, Journal of Lubrication Technology,* Series F, Vol. 92, 1970, pp. 155–162.

[4] Dawson, D. and Higginson, G. R., *Elastohydrodynamic Lubrication,* Pergamon Press, New York, 1966.

[5] Gear, C. W., *Numerical Initial Value Problems in Ordinary Differential Equations,* Prentice Hall, Englewood Cliffs, N.J., 1971.

[6] Gu, A., "An Improved Method for Calculating the Spin Torque in Fully Lubricated Ball Race Contact," *ASME Transactions, Journal of Lubrication Technology,* Series F, Vol. 95, 1973, pp. 106–108.

[7] Harris, T. A., "Ball Motion in Thrust Loaded Angular Contact Bearings with Coulomb Friction," *ASME Transactions, Journal of Lubrication Technology,* Series F, Vol. 93, 1971, pp. 32–38.

[8] Harris, T. A., "An Analytical Method to Predict Skidding in Thrust Loaded Angular Contact Ball Bearings," *ASME Transactions, Journal of Lubrication Technology,* Series F, Vol. 93, 1971, pp. 17–24.

[9] Harris, T. A., *Rolling Bearing Analysis,* Wiley, New York, 1966.

[10] Hirano, F., "Motion of a Ball in Angular-Contact Ball Bearings," *ASLE Transactions,* Vol. 8, 1965, pp. 425–434.

[11] Johnson, K. L. and Cameron, R., "Shear Behavior of Elastohydrodynamic Oil Film at High Rolling Contact Pressures," *Proceedings of the International Mechanical Engineers Society,* Vol. 182, London, 1967–1968, pp. 307–330.

[12] Jones, A. B., "Ball Motion and Sliding Friction in Ball Bearings," *ASME Transactions, Journal of Basic Engineering,* Series D, Vol. 81, 1959, pp. 1–12.

[13] Jones, A. B., "A General Theory for Elastically Constrained Ball and Radial Roller Bearings Under Arbitrary Load and Speed Conditions," *ASME Transactions, Journal of Basic Engineering,* Series D, Vol. 82, 1960, pp. 309–320.

[14] McGrew, J. M., Gu, A., Cheng, H. S., and Murray, S. F., "Elastohydrodynamic Lubrication—Preliminary Design Manual," Tech. Rept AFAPL-TR-70-27, 1970, Air Force Aero Propulsion Lab, Wright-Patterson Air Force Base, Ohio.

[15] Poplawski, J. V. and Mauriello, J. A., "Skidding in Lightly Loaded High-Speed Ball Thrust Bearings," ASME Paper 69-LUBS-20, San Francisco, Calif., June 1969.

[16] Smith, R. L., Walowit, J. A., and McGrew, J. M., "Elastohydrodynamic Traction Characteristics of 5P4E Polyphenyl Ether," *ASME Transactions, Journal of Lubrication Technology,* Series F, Vol. 95, 1973, pp. 353–362.

[17] Smith, R. L., Walowit, J. A., Gupta, P. K., and McGrew, J. M., "Research on Elastohydrodynamic Lubrication of High Speed Rolling-Sliding Contacts," Tech. Rept AFAPL-TR-72-56, 1972, Air Force Aero Propulsion Lab., Wright-Patterson Air Force Base, Ohio.

[18] Walters, C. T., "The Dynamics of Ball Bearings," *ASME Transactions, Journal of Lubrication Technology,* Series F, Vol. 93, 1971, pp. 1–10.